

Received February 18, 2020, accepted March 4, 2020, date of publication March 9, 2020, date of current version March 24, 2020.

Digital Object Identifier 10.1109/ACCESS.2020.2979483

# Planar Monopole Antenna With a Parasitic Shorted Strip for Multistandard Handheld Terminals

AIXIN CHEN<sup>ID</sup>, MINGYU SUN, ZHE ZHANG, AND XUEDONG FU

School of Electronic and Information Engineering, Beihang University, Beijing 100191, China

Corresponding author: Aixin Chen (axchen@buaa.edu.cn)

This work was supported in part by the National Natural Science Foundation of China under Grant 61371006, in part by the Domain Foundation of Equipment Advance Research under Grant 61409220209, in part by the National Defense Science and Technology Innovation Zone Project, and in part by the Equipment Advance Research Project.

**ABSTRACT** A planar monopole antenna with a parasitic shorted strip for multistandard handheld terminal is presented. The proposed antenna simply consists of two overlapping strips: a long strip on the front side and a parasitic shorted strip on the back side. To make the proposed antenna easy to manufacture and reduce the manufacturing cost, the entire structure is fully printed without VIA holes, the long strip monopole is directly fed, and the parasitic shorted strip is coupled-fed by the overlapped part. For lower and middle frequencies, the GSM900 and PCS bands are excited by the fundamental mode of the long strip and the parasitic shorted strip, respectively. For the upper frequency, the Wi-Fi2400/RFID2450 and LTE2300/2500 bands are provided by the third-order mode of the long strip. The detailed design of the proposed antenna and its radiation performances are studied. The proposed multiband antenna occupies a small area of  $40 \times 18 \text{ mm}^2$  on a printed circuit board (PCB). The measured results show that the proposed antenna has three impedance bands with return loss less than  $-6 \text{ dB}$ : 25.6% for the low band (850–1100 MHz), 13.3% for the middle band (1750–2000 MHz) and 22.7% for the high band (2190–2750 MHz).

**INDEX TERMS** Planar monopole antenna, parasitic shorted strip, coupled-fed, handheld terminals, multi-band operation.

## I. INTRODUCTION

Promising multiband, small internal antennas suitable for multistandard handheld terminals have been reported recently. The antenna structures include PIFA or printed PIFA [1]–[3], printed or folded loop [4]–[7], planar or fractal monopole [8]–[12], and slot antennas [13]. Among those antennas, the planar monopole antenna is most attractive due to its thin size, compact size, broadband characteristics and ease of manufacture.

To meet diverse communication needs, multistandard antennas have received widespread attention in recent years. Multiband technology and wideband technology have been applied to these antennas [14]. A variety of techniques have been applied to multistandard handheld terminal antennas. The key concept of multiband technology is to flexibly design the physical radiation structural model of a single

antenna, using parasitic elements, multiple strips, or higher-order mode excitation to enable the antenna to excite multiple resonance modes. Multiple strips can provide multibands [15], [16]. Folded strips with additional straight strips are introduced in [17] to excite more modes for bandwidth enhancement. Parasitic elements were introduced to improve the performance of an antenna or act as an extra radiator [17]–[19]. For example, in [15] driven monopoles with multiple branches and parasitic ground strips were applied simultaneously for multiband operation. A stair-like branch etched on the ground was used as a parasitic patch fed by coupling for multistandard antenna in [18]. To obtain good impedance matching, a coupled feed was adopted in [17] and [18], but a directed feed matching element was used in [19].

In this paper, we demonstrate a planar monopole antenna with a parasitic shorted strip for multistandard handheld terminals. The antenna is formed by a long strip monopole on the front side and a parasitic shorted strip on the back side, and portion of each spatially overlaps. The long strip

The associate editor coordinating the review of this manuscript and approving it for publication was Shah Nawaz Burokur<sup>ID</sup>.

**TABLE 1.** Comparison of the performance of multi-standard antennas.

Ref.	Dimension (mm <sup>3</sup> )	-6 dB Bandwidth (MHz)	Gain (dBi)
[10]	68×15×0.8	698-1046	0.4-2.8
		1618-2703	1.9-4.3
		3018-4377	2.4-4.4
		4697-6000	4.3-5.6
[14]	80×8×5.8	690-980 1630-2740	0.3-3.0 3.1-5.6
[15]	60×15×0.8	660-1065 1665-3000	0.5-2.0 0.5-3.0
[17]	20×15×0.8	810-980 1710-2700	0.8-1.8 1.6-2.6
[18]	56×5×5.8	690-1000	2.6-5.2
		1680-2950	1.3-4.0
This work	40×18×1	850-1100	1.9-2.6
		1750-2000	2.0-3.0
		2190-2750	3.4-4.3

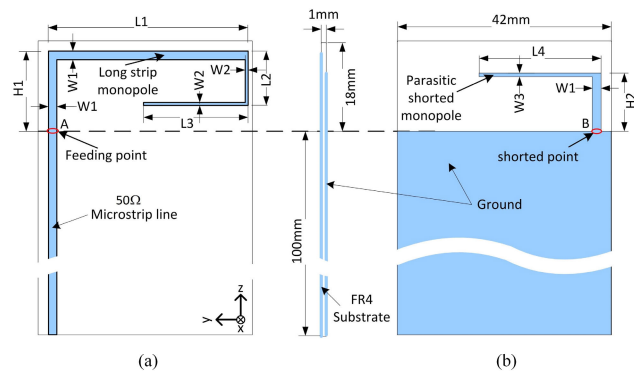


**FIGURE 1.** Configuration of the proposed planar monopole antenna. (a) Top view, (b) bottom view.

monopole is the main radiator contributing a fundamental mode and a third-order mode, and as an extra radiator, the parasitic shorted strip on the back side contributes another fundamental mode. The long strip monopole is directly fed and the parasitic shorted strip is coupled-fed by the overlapped part. The entire structure is fully printed without VIA holes. Table.1 compares the figures of merit (including the ground clearance dimensions,-6 dB bandwidth, gain) of multistandard antennas in the references. The proposed antenna can cover several standard bands including GSM900 (890-960 MHz), PCS (1850-1990 MHz), Wi-Fi2400 (2412-2484 MHz), RFID2450 (2400-2483.5 MHz) and LTE2300/2500 (2305-2400 MHz/2500-2690 MHz).

**II. THE PROPOSED ANTENNA**

The configuration of the proposed planar monopole antenna is illustrated in Fig. 1. A 1.0 mm-thick FR-4 substrate ( $\epsilon_r = 4.4$ ) with a size of  $118 \times 42 \text{ mm}^2$  is used as the system circuit board of the handheld terminal. On its back side, the ground plane is  $100 \times 42 \text{ mm}^2$ . The radiating elements of the antenna are printed on a small nonground area of  $17 \times 39 \text{ mm}^2$  on both sides of the board.

Fig. 1(a) shows the top view of the proposed antenna. A long winding strip monopole and a  $50 \Omega$  microstrip line are printed on the front side. They are connected at feeding point

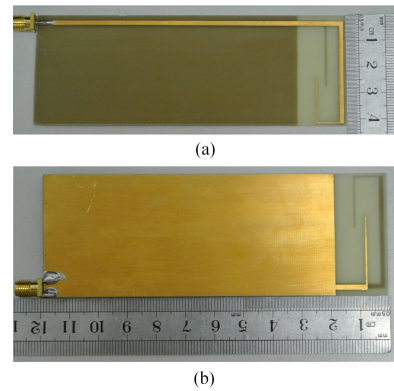


**FIGURE 2.** Photograph of the fabricated prototype, (a) top view, (b) bottom view.

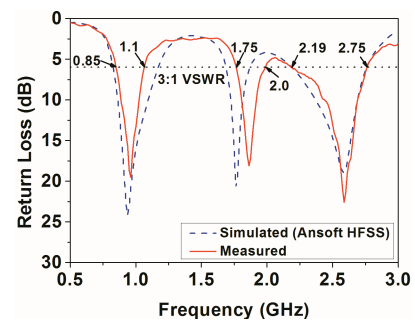


**FIGURE 3.** Measured and simulated return loss of the proposed antenna.

A. Fig. 1(b) shows the bottom view. An inverted L parasitic shorted strip and a system ground plane are printed on the back side. They are connected at the shorted point B. The antenna has a simple structure, and its radiators only occupy small areas on the front and back sides of the no-ground portion, leaving a large unoccupied region for possible system elements.

Table. 2 shows the dimensions of the antenna. The radiating patch consists of a long strip monopole on the top layer and a parasitic shorted strip on the bottom layer. There is a linear relationship between the length of the strip and the resonance wavelength. The total length of the long strip monopole is 84 mm ( $H1+L1+L2+L3$  in Fig. 1(a)), which is approximately a quarter of the wavelength of 960 MHz. The long strip monopole can excite two modes: one is a fundamental mode with a quarter wavelength at approximately 960 MHz, and the other is a third-order mode with a three-quarter wavelength at approximately 2590 MHz providing the GSM900/Wi-Fi2400/RFID2450/ LTE2300/2500 operation bands. Resonance frequencies can be changed by tuning the length of the long strip. The total length of the parasitic shorted strip on the back side is 36.5 mm ( $H2+L4$ ), which is approximately a quarter wavelength at 1860 MHz. It generates a fundamental resonance at approximately 1860 MHz to cover the PCS operation band. Tuning the length of the parasitic shorted strip alters its resonance frequency. The widths of the two strips are segmentedly changed to obtain good

TABLE 2. Optimized antenna dimensions (unit: mm).

Parameters	(mm)	Parameters	(mm)	Parameters	(mm)
L1	39	L2	10	L3	18
L4	25.5	W1	1.8	W2	0.5
W3	0.7	H1	17	H2	11

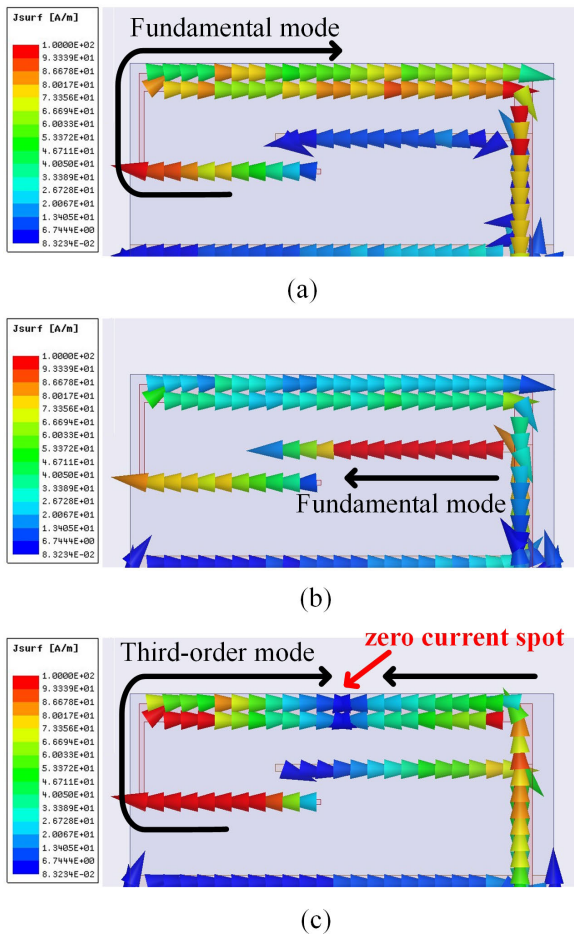


FIGURE 4. Simulated vector current distributions on the proposed antenna at different frequencies, (a) 960 MHz, (b) 1860 MHz, (c) 2590 MHz.

impedance matching. More detailed effects of the dimensions of the proposed antenna will be illustrated in Fig. 6 and Fig. 7 in the next section.

### III. RESULTS AND DISCUSSION

The proposed antenna is fabricated and tested. The prototype is shown in Fig. 2. A 50 Ω microstrip line is connected with a 50 Ω SMA for testing. Fig. 3 shows the measured and simulated return loss for the proposed antenna with the dimensions given in Table. 1. The simulated result is obtained using Ansoft HFSS. The measured result agrees well with the simulated result except for a small shift at the second resonance. As discussed in section II, three desired resonances at approximately 960 MHz, 1860 MHz and 2590 MHz are excited, and good impedance matching is obtained. According to the definition of a 3:1 VSWR or a return loss of 6 dB, the first resonance indicates a wide

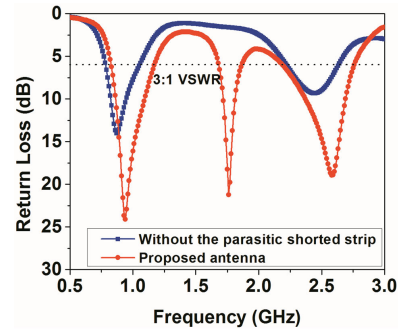


FIGURE 5. Comparison of return loss for the antennas with and without the parasitic shorted strip.

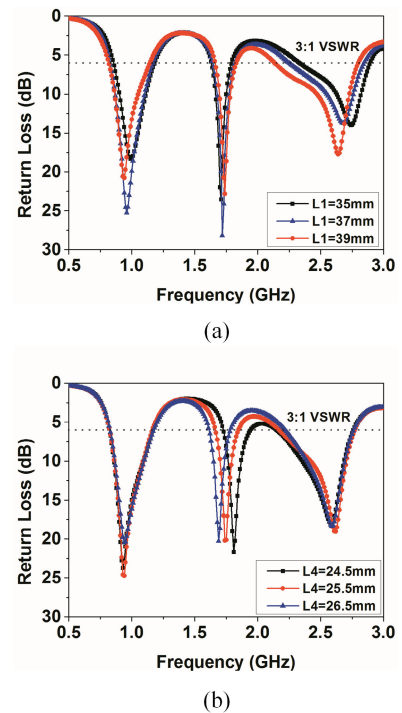
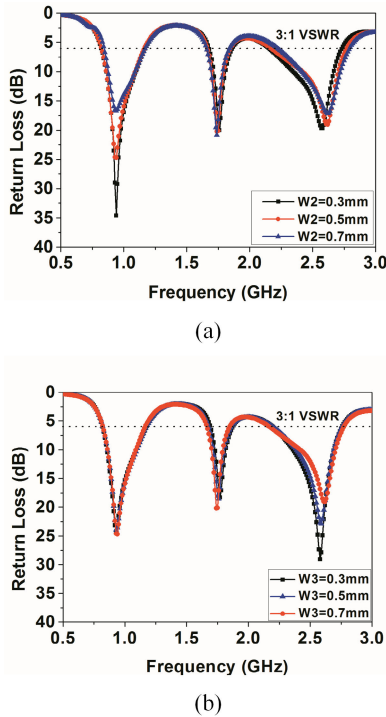


FIGURE 6. Simulated return loss as a function of lengths L1 and L4; (a) the long strip length L1, (b) the parasitic shorted strip length L4. Other dimensions are the same as those given in Table 1.

bandwidth of 250 MHz (850 MHz-1100 MHz), covering the GSM900 operation. The second resonance has a bandwidth of 250 MHz (1750 MHz-2000 MHz), covering the PCS operation. The third resonance shows an even wider bandwidth of 560MHz (2190 MHz-2750 MHz), which covers the Wi-Fi2400/RFID2450/LTE2300/2500 operation.

To better understand the multiband principles of the proposed antenna, the simulated vector current distributions at 960, 1860, and 2590 MHz (frequencies with the best impedance matching in the above three bands) are shown in Fig. 4. At 960 MHz and 2590 MHz in Figs. 4(a) and (c), a stronger current is found in the long strip, which means that the long strip monopole is the main radiator at these two frequencies. It is obvious from the current distribution that the fundamental mode is excited at 960 MHz, while



**FIGURE 7.** Simulated return loss as a function of widths  $W_2$  and  $W_3$ ; (a) the long strip width  $W_2$ , (b) the parasitic shorted strip width  $W_3$ . Other dimensions are the same as those given in Table 1.

the third-order mode with a zero current spot is excited at 2590 MHz. Similarly, at 1860 MHz in Fig.4(b), a stronger current is found in the parasitic shorted strip, which means that the parasitic shorted strip is the main radiator at this frequency, and the fundamental mode is excited in this operating band.

To more clearly reveal the contributions of the long strip and the parasitic strip to the antenna, a reference antenna is simulated. It has almost the same configuration as that of the proposed antenna except for the parasitic shorted strip. Fig. 5 shows a comparison of the return loss of the proposed antenna and the reference antenna, which indicates that the reference antenna has a fundamental resonance at approximately 870 MHz and a high-order resonance at approximately 2440 MHz. For the proposed antenna, by embedding the parasitic shorted strip, an extra resonance at approximately 1860 MHz is obtained. Meanwhile, the lower and the higher resonances are within the same bands as those of the reference antenna. A small difference is that these resonances are shifted to higher frequencies in the proposed antenna, and their bandwidths are improved.

The dimensions of the antenna determine its characteristics. The resonance frequencies of the two strips are mainly determined by their respective lengths. The effects of the long strip length  $L_1$  on the return loss are depicted in Fig. 6(a). When  $L_1$  increases from 35 mm to 39 mm, the fundamental and high-order resonances of the long strip monopole are shifted to the lower frequency, but the resonance frequency

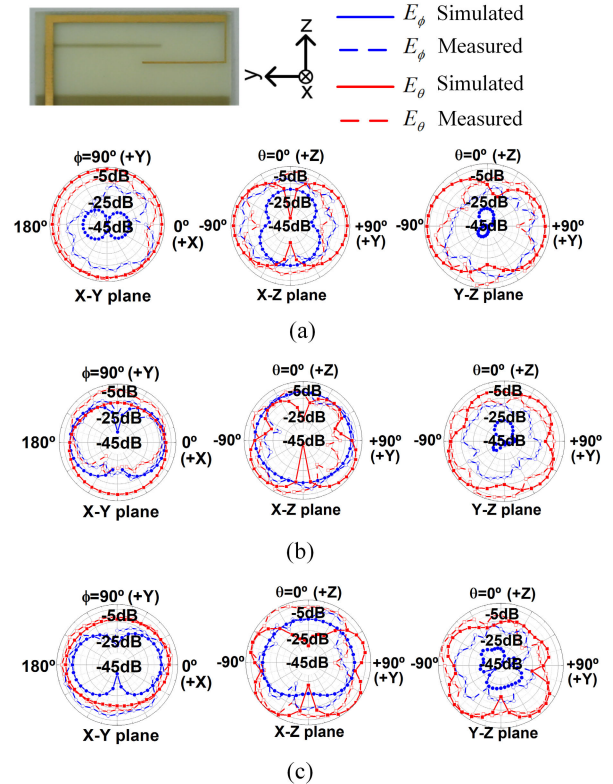


**FIGURE 8.** Simulated and measured radiation patterns of the proposed antenna at (a)960 MHz, (b)1860 MHz, and (c)2590 MHz.

of the parasitic shorted strip is hardly affected. The effects of the parasitic shorted strip length  $L_4$  are analyzed in Fig. 6(b). When  $L_4$  varies from 24.5 mm to 26.5 mm, the resonance of the parasitic shorted strip is shifted to the lower frequency, but the fundamental and the high-order resonances of the long strip monopole are affected slightly.

The width of the strip mainly affects the impedance matching of the proposed antenna. As shown in Fig. 7(a), when the long strip width  $W_2$  increases from 0.3 mm to 0.7 mm, the impedance matching of the long strip monopole becomes worse. The fundamental resonance varies significantly and the high-order resonance varies slightly. However, the resonance of the parasitic shortened strip is hardly affected. In Fig. 7(b), when the parasitic shorted strip width  $W_3$  increases from 0.3 mm to 0.7 mm, the impedance matching of the parasitic shorted strip is improved slightly. At the same time, the fundamental resonance of the long strip monopole is hardly affected, but in the high-order resonance, it becomes obviously worse.

Fig. 8 demonstrates the measured co-polarization and cross-polarization radiation patterns of the proposed antenna at 960 MHz, 1860 MHz and 2590 MHz. It can be seen that good omni-directional radiation performances are obtained in the X-Y plane both in simulation and measurement. A monopole-like radiation pattern is seen at 960 MHz. For 1860 MHz and 2590 MHz, more variation and some nulls are found in the radiation patterns.

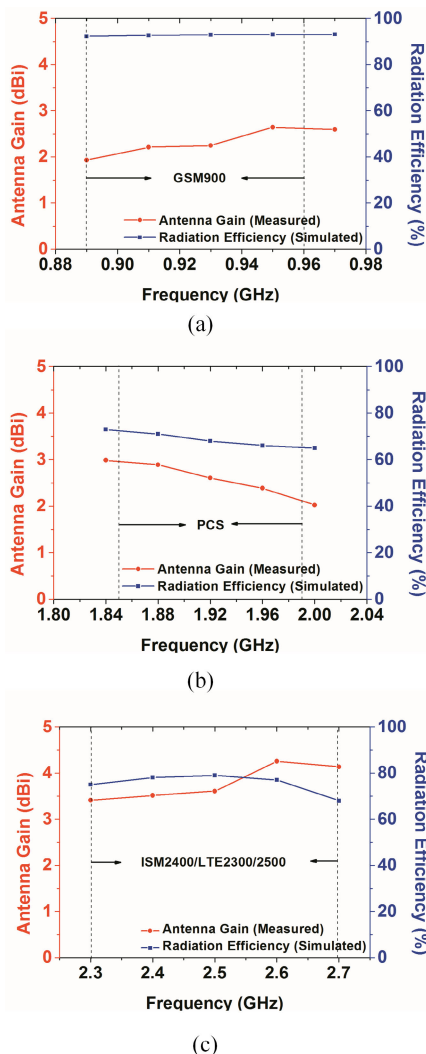


FIGURE 9. Measured antenna gains and simulated radiation efficiencies of the proposed antenna.

Fig. 9 presents the measured antenna gains and the simulated radiation efficiencies. For frequencies within the GSM900 operation band, the measured antenna gain is approximately 1.9 - 2.6 dBi, while the simulated radiation efficiency is approximately 92 - 94%. For frequencies in the PCS operation band, the measured antenna gain is approximately 2.0 - 3.0 dBi, while the simulated radiation efficiency is approximately 65 - 73%. For frequencies covering the Wi-Fi2400/RFID2450/LTE2300/2500 operation bands, the measured antenna gain is approximately 3.4 - 4.3 dBi, while the simulated radiation efficiency is approximately 68 - 79%. The radiation performance of the proposed antenna is acceptable for practical applications.

IV. EFFECTS OF HUMAN ON ANTENNA PERFORMANCE

The effects of proximity environment is discussed in this section. Head and hand models are used for SAR calculation [10], [20]. As illustrated in Fig. 10, the proposed antenna

TABLE 3. Simulated SAR values for 10-g head issue.

Frequency (MHz)	Input power (dBm)	S11 (dB)	10-g SAR (W/kg)
960	24	-7.06	1.10
1860	21	-5.30	0.26
2590	21	-16.21	0.24

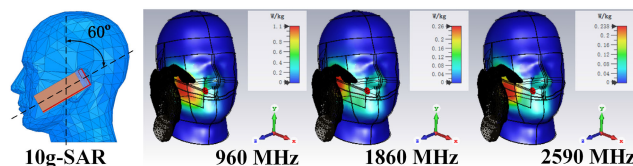


FIGURE 10. SAR simulation model (CST) for the proposed antenna.

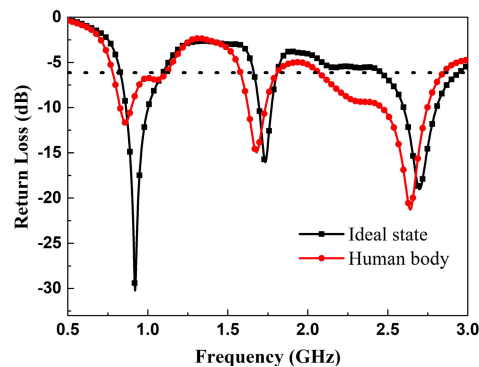


FIGURE 11. Simulated return loss with human body.

is oriented by 60° to the vertical line of the phantom head. This distance between the ground and the phantom ear is 5 mm. In SAR calculation, the simulated input power is 24 dBm at 960 MHz, 21 dBm at 1860 MHz, 2590 MHz. Table. 3 lists the simulated SAR value for 10g-head tissues at desired frequencies. It can be seen that, all the SAR values are less than 2.0 W/kg. The simulated return loss of the human body model is shown in Fig. 11. Simulation results show that the frequency band is not significantly degraded due to changes in the external environment, which make the antenna suitable for mobile multistandard phone antenna.

V. CONCLUSION

A planar monopole antenna for multiband applications is presented. The radiating elements of the proposed antenna occupy an area of 17 × 39 mm<sup>2</sup> on the system circuit board. It has a simple structure, which only consists of two strips. One long strip monopole on the front side generates two resonances and one parasitic shorted strip on the back side as an extra radiator generates another resonance. Three good impedance matching bands are obtained. The proposed antenna is suitable for GSM900/ PCS/Wi-Fi2400/RFID2450/LTE2300/2500 operation. Because this antenna is fully printed with no VIA-hole, it is easy and inexpensive to manufacture. The simple structure and good radiation characteristics make the proposed antenna attractive for practical applications.

## REFERENCES

- [1] A. J. Alazemi and G. M. Rebeiz, "A tunable single-feed triple-band LTE antenna with harmonic suppression," *IEEE Access*, vol. 7, pp. 104667–104672, 2019.
- [2] H. F. AbuTarboush, R. Nilavalan, T. Peter, and S. W. Cheung, "Multi-band Inverted-F antenna with independent bands for small and slim cellular mobile handsets," *IEEE Trans. Antennas Propag.*, vol. 59, no. 7, pp. 2636–2645, Jul. 2011.
- [3] L. Pazin and Y. Leviatan, "Narrow-size multiband Inverted-F antenna," *IEEE Antennas Wireless Propag. Lett.*, vol. 10, pp. 139–142, 2011.
- [4] S.-W. Su, C.-T. Lee, and S.-C. Chen, "Compact, printed, tri-band loop antenna with capacitively-driven feed and end-loaded inductor for notebook computer applications," *IEEE Access*, vol. 6, pp. 6692–6699, 2018.
- [5] D. Wu, S. W. Cheung, and T. I. Yuk, "A compact and low-profile loop antenna with multiband operation for ultra-thin smartphones," *IEEE Trans. Antennas Propag.*, vol. 63, no. 6, pp. 2745–2750, Jun. 2015.
- [6] H. Xu, H. Wang, S. Gao, H. Zhou, Y. Huang, Q. Xu, and Y. Cheng, "A compact and low-profile loop antenna with six resonant modes for LTE smartphone," *IEEE Trans. Antennas Propag.*, vol. 64, no. 9, pp. 3743–3751, Sep. 2016.
- [7] H. Wang, Y. Wang, J. Wu, P. Chen, Z. Wu, C.-Y.-D. Sim, and G. Yang, "Small-size reconfigurable loop antenna for mobile phone applications," *IEEE Access*, vol. 4, pp. 5179–5186, Jul. 2016.
- [8] W. Jiang, Y. Cui, B. Liu, W. Hu, and Y. Xi, "A dual-band MIMO antenna with enhanced isolation for 5G smartphone applications," *IEEE Access*, vol. 7, pp. 112554–112563, 2019.
- [9] M. Samsuzzaman, M. T. Islam, and M. J. Singh, "A compact printed monopole antenna with wideband circular polarization," *IEEE Access*, vol. 6, pp. 54713–54725, 2018.
- [10] X. Wang, Y. Wu, W. Wang, and A. A. Kishk, "A simple multi-broadband planar antenna for LTE/GSM/UMTS and WLAN/WiMAX mobile handset applications," *IEEE Access*, vol. 6, pp. 74453–74461, 2018.
- [11] K.-L. Wong, W.-Y. Chen, and T.-W. Kang, "On-board printed coupled-fed loop antenna in close proximity to the surrounding ground plane for pentaband WWAN mobile phone," *IEEE Trans. Antennas Propag.*, vol. 59, no. 3, pp. 751–757, Mar. 2011.
- [12] D. V. Navarro-Mendez, L. F. Carrera-Suarez, E. Antonino-Daviu, M. Ferrando-Bataller, M. Baquero-Escudero, M. Gallo, and D. Zamberlan, "Compact wideband Vivaldi monopole for LTE mobile communications," *IEEE Antennas Wireless Propag. Lett.*, vol. 14, pp. 1068–1071, 2015.
- [13] F.-H. Chu and K.-L. Wong, "Internal coupled-fed dual-loop antenna integrated with a USB connector for WWAN/LTE mobile handset," *IEEE Trans. Antennas Propag.*, vol. 59, no. 11, pp. 4215–4221, Nov. 2011.
- [14] Y. Wang and Z. Du, "Wideband monopole antenna with less nonground portion for octa-band WWAN/LTE mobile phones," *IEEE Trans. Antennas Propag.*, vol. 64, no. 1, pp. 383–388, Jan. 2016.
- [15] C. Deng, Y. Li, Z. Zhang, and Z. Feng, "Planar printed multi-resonant antenna for octa-band WWAN/LTE mobile handset," *IEEE Antennas Wireless Propag. Lett.*, vol. 14, pp. 1734–1737, 2015.
- [16] Y. Yang, Z. Zhao, W. Yang, Z. Nie, and Q.-H. Liu, "Compact multimode monopole antenna for metal-rimmed mobile phones," *IEEE Trans. Antennas Propag.*, vol. 65, no. 5, pp. 2297–2304, May 2017.
- [17] G.-H. Kim and T.-Y. Yun, "Small wideband monopole antenna with a distributed inductive strip for LTE/GSM/UMTS," *IEEE Antennas Wireless Propag. Lett.*, vol. 14, pp. 1677–1680, Mar. 2015.
- [18] Y. Liu, Y. Luo, and S. Gong, "An antenna with a stair-like ground branch for octa-band narrow-frame mobile phone," *IEEE Antennas Wireless Propag. Lett.*, vol. 17, no. 8, pp. 1542–1546, Aug. 2018.
- [19] W.-S. Chen and W.-C. Jhang, "A planar WWAN/LTE antenna for portable devices," *IEEE Antennas Wireless Propag. Lett.*, vol. 12, pp. 19–22, 2013.
- [20] C. Deng, Z. Xu, A. Ren, and S. V. Hum, "TCM-based bezel antenna design with small ground clearance for mobile terminals," *IEEE Trans. Antennas Propag.*, vol. 67, no. 2, pp. 745–754, Feb. 2019.



**AIXIN CHEN** received the Ph.D. degree in electromagnetic field and microwave technology from the University of Electronic Science and Technology of China, Chengdu, China, in 1999. From 2000 to 2002, he was a Postdoctoral Fellow with the School of Electronic Information and Engineering, Beihang University, Beijing, China, where he is currently a Professor. His research interests mainly include antennas and electromagnetic compatibility.



**MINGYU SUN** received the B.S. degree from the School of Physics, Dalian University of Technology, Dalian, China, in 2017. He is currently pursuing the M.S. and Ph.D. degrees with the School of Electronic and Information Engineering, Beihang University, Beijing, China.

His main research interests include reconfigurable antenna, reconfigurable metasurface, and electromagnetic absorber.



**ZHE ZHANG** received the B.S. degree in electrical engineering from the Nanjing University of Aeronautics and Astronautics, Nanjing, China, in 2012, and the M.S. degree in electrical engineering from Lanzhou University, Lanzhou, China, in 2016. He is currently pursuing the Ph.D. degree with the School of Electronics and Information Engineering, Beihang University, Beijing.

His current research interests include metamaterials based on antenna and airborne antenna.



**XUEDONG FU** received the B.S. and M.S. degrees in electronic science and technology from the China University of Mining and Technology, Xuzhou, China, in 2015 and 2018, respectively. He is currently pursuing the Ph.D. degree with the School of Electronics and Information Engineering, Beihang University, Beijing.

His current research interests include differential antenna and electromagnetic compatibility.

• • •